Proc. Natl. Acad. Sci. USA
Vol. 93, pp. 1853–1858, March 1996
Neurobiology

The multiple phenotypes of allosteric receptor mutants

(nicotinic acetylcholine receptor/glycine receptor/ion channel/neurotransmitter site)

JEAN-LUC GALZI*†, STUART J. EDELSTEIN‡, AND JEAN-PIERRE CHANGEUX*

*Centre National de la Recherche Scientifique Unité de Recherche Associée D1284, Neurobiologie Moléculaire, Institut Pasteur 75734, Paris Cedex 15, France; and ‡Department of Biochemistry, University of Geneva, CH-1211 Geneva 4, Switzerland

Contributed by Jean-Pierre Changeux, October 30, 1995

ABSTRACT **Channel-linked neurotransmitter receptors are membrane-bound heterooligomers made up of distinct, although homologous, subunits. They mediate chemo–electrical signal transduction and its regulation via interconversion between multiple conformations that exhibit distinct pharmacological properties and biological activities. The large diversity of functional properties and the widely pleiotropic phenotypes, which arise from point mutations in their subunits (or from subunit substitutions), are interpreted in terms of an allosteric model that incorporates multiple discrete conformational states. The model predicts that three main categories of phenotypes may result from point mutations, altering selectively one (or more) of the following features: (*i*) the properties of individual binding sites (*K* phenotype), (*ii*) the biological activity of the ion channel (γ phenotype) of individual conformations, or (*iii*) the isomerization constants between receptor conformations (*L* phenotype). Several nicotinic acetylcholine and glycine receptor mutants with complex phenotypes are quantitatively analyzed in terms of the model, and the analogies among phenotypes are discussed.**

Ligand-gated ion channels (1–4) mediate rapid communication between neurons and their target cells via a fast permeability response to a brief high concentration pulse of neurotransmitter released by the nerve ending in the synaptic cleft; in addition, a prolonged exposure to the neurotransmitter results in a slow and reversible decline of the amplitude of the ionic response to the neurotransmitter (5–7) via stabilization of a refractory desensitized state. Ligand-gated ion channels share several properties with classical allosteric regulatory proteins (8–10). (*i*) They possess an oligomeric quaternary structure. (*ii*) Their biologically active site, the ion channel located in the axial cleft, opens in an all-or-nothing manner. (*iii*) They carry several categories of topographically distinct regulatory sites that differentially recognize agonists or competitive and noncompetitive antagonists as positive or negative allosteric effectors. (*iv*) They undergo conformational transitions between discrete interconvertible states with distinct ligand affinities and biological activities (1).

But receptor channels also display specific features not found among allosteric enzymes (11). First, they may form heterooligomers from distinct, although homologous, subunits pseudo-symmetrically arranged around a unique rotational axis perpendicular to the plane of the membrane; as a consequence, the neurotransmitter-binding sites, located at subunit boundaries, are only partially equivalent but, nevertheless, interact in a positively homotropic manner. Second, they have access to more than two discrete conformational states; muscle and electric organ nicotinic receptors, for instance, may interconvert between four conformations with kinetics extending from the microsecond to the minute time scale. Finally, in addition to these rather unconventional properties, point mutations within their subunit genes often result in "complex" and extremely pleiotropic phenotypes with, for instance, concomitant modifications of the apparent affinity for agonist, channel properties, and agonist-versus-antagonist specificity.

Since the discovery (12–19) of these mutations, the interpretation of their complex phenotype in molecular terms has become a challenging issue. We have therefore reexamined the classical allosteric model proposed for nicotinic acetylcholine receptors (1, 6) and show here that the allosteric scheme offers plausible and experimentally verifiable interpretations for these complex phenotypes. We also consider the classical sequential model (20) and critically compare its specific predictions to those of the allosteric model.

THE ALLOSTERIC MODEL RECONSIDERED

Biological Premises

The model rests upon the following biological premises:

Multiplicity of the Phenotypes. Biochemical and biophysical studies on recombinant ligand-gated ion channels show that various combinations of wild-type (WT) or mutant subunits result in receptor molecules with a wide diversity of binding, signal transduction, and possibly folding phenotypes. These diverse oligomers display distinct pharmacological specificities (21, 22), conductance and ionic selectivities (23), kinetics of activation and desensitization (14, 24, 25), and a variable number of conducting (12, 26) or desensitized (6, 27) states.

Pleiotropy of the Phenotypes. Mutations of amino acids directly contributing to the major functional sites of ligand-gated ion channels (neurotransmitter sites, ion channel, and allosteric regulatory sites) frequently alter not only the ligand-binding properties of the mutated site but also signal transduction and its regulation in the oligomer. For example, a single mutation in the M2 channel domain of the α7 nicotinic acetylcholine receptor, Leu-247 → Thr (12–14), yields a receptor that is insensitive to the channel blocker QX222, has lost desensitization, and displays an apparent affinity for acetylcholine up to 200-fold higher than for WT. In addition, the mutant receptor exhibits two conducting states activated by high (the 40-pS state) versus low (the 80-pS state) concentrations of acetylcholine; moreover, a competitive antagonist of the WT receptor, dihydro-β-erythroidine (DHβE), behaves on this mutant as a full agonist (with 10-fold higher apparent affinity than acetylcholine) and exclusively activates the high conductance state.

Analogy Among the Phenotypes. Mutations at several different positions along the primary sequence of receptor subunits may produce similar, although not identical, phenotypes. For instance, shifts in the neurotransmitter dose–response

The publication costs of this article were defrayed in part by page charge payment. This article must therefore be hereby marked "*advertisement*" in accordance with 18 U.S.C. §1734 solely to indicate this fact.

Abbreviations: WT, wild type; DHβE, dihydro-β-erythroidine.

†Present address: Centre National de la Recherche Scientifique UPR 9050, Département Récepteurs et Protéines Membranaires, Ecole Supérieure des Biotechnologies, 67400 Illkirch, France.

curve are obtained by mutating amino acids contributing to either the ligand-binding domain (22, 28–31) or to the ion-channel domain (12–19), even though they are located 20–40 Å away from each other in nicotinic receptors (32). A particularly striking case of analogy among phenotypes of $\alpha 7$ nicotinic receptor mutants altered in the M2 channel domain is discussed below.

Restatement of the Model

The model rests upon the following assumptions (Fig. 1):

(*i*) Receptor molecules exist in several (at least three) *discrete* conformations, S_i, which correspond to thermodynamically stable states with defined tertiary and quaternary structures. These conformations are qualitatively described by a structural parameter Σ_i and functionally defined as closed (but activatable), active (channel open), and desensitized (closed but refractory). Each state is characterized by its affinity for the agonist (K_i) or other ligands, and its conductance (γ_i, in pS).

(*ii*) The interconversion between any two conformational states S_i and S_j occurs freely with an allosteric equilibrium constant ${}^{ij}L = [S_j]/[S_i]$, and ligands stabilize the conformations to which they bind with higher affinity.

(*iii*) One receptor oligomer, with a given subunit composition, has access to a unique set of conformational states, possibly including more than one conducting (glycine receptors, ref. 26) or desensitized (nicotinic receptors, refs. 6, 27) state.

(*iv*) Substituting one subunit for another, or mutating amino acids in one (or more) subunit(s), may alter the pattern of the conformational network by changing the intrinsic binding properties or the biological activity (conductance) of one or more conformation or changing the equilibrium constants between conformational states. In addition, the number of conformational states may vary—i.e., certain conformations may become virtually inaccessible, or conversely, stable.

The mechanistic and mathematical formulation used is given by Monod, Wyman, and Changeux (8) for allosteric proteins with extension to multiple-states equilibria (1, S.J.E., O. Schaad, E. Henry, D. Bertrand, J.-P.C., unpublished work). The equations (in legends) used in the present work are developed for a two- (see Figs. 2 and 3) or three- (see Fig. 4) state scheme of channel activation or ligand binding.

PHENOTYPIC CHANGES IN ALLOSTERIC NETWORKS CAUSED BY POINT MUTATIONS

Theoretical Predictions

For simplicity, in all cases considered in this section and unless otherwise specified, both the WT and mutant receptors are assumed to interconvert to the same finite number of identical quaternary structures. Also, as kinetics of activation and desensitization take place over significantly different time scales (desensitization is generally slow compared to activation), the conformational scheme used to describe receptor activation is, in a first approximation, reduced to only those interconverting states involved in the activation process (resting and active states). Taking into account the intrinsic properties of individual conformational states and their possibilities to isomerize to other conformational states (Fig. 1), three main classes of effects may be expected in such an allosteric system with increasing numbers of interconverting states.

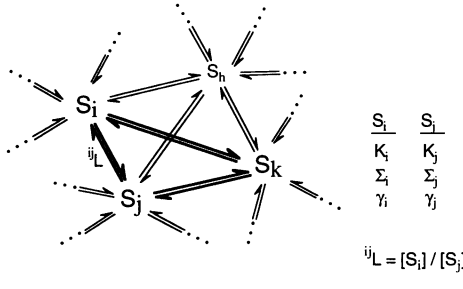

FIG. 1. The allosteric network. Receptor molecules exist in multiple conformational states. Each conformation S_i corresponds to a unique quaternary structure (Σ_i) with intrinsic binding properties (K_i) and biological activity (γ_i). The interconversion between any two conformational states S_i and S_j is described by an allosteric equilibrium constant ${}^{ij}L = [S_j]/[S_i]$.

The Binding or *K* Phenotype. The *K* phenotype is assumed to result from mutations that selectively alter the *intrinsic* binding affinities of individual conformational states. In this context two possibilities may be envisioned. First, the affinity of each conformation changes but the affinity ratio (${}^{ij}c = K_i/K_j$) between conformations remains constant. The apparent affinity (EC_{50}) for response activation would then change with neither modifications of cooperativity (Hill coefficient) nor response amplitude (Fig. 2). In other words, the dose–response curves are parallel. Second, the mutation selectively alters the affinity of certain states only, leading to changes in the affinity ratios (${}^{ij}c$). In this case, not only would the apparent affinity be affected but also cooperativity and, possibly, response amplitude (Fig. 2). Furthermore, as *c* increases, agonists may progressively become partial agonists or even competitive antagonists. Finally, for none of the *K* phenotypes would the spontaneous equilibrium between any states S_i and S_j be altered in the absence of ligand.

Isomerization or *L* Phenotype. The *L* phenotype is assumed to result from mutations that selectively alter the equilibrium constant between two given interconvertible conformations. The intrinsic properties of each conformation—i.e., the microscopic binding constants and the state of channel activity, are further assumed to remain unchanged. Let us consider a *two-state* model consisting of an inactive (channel closed) B and an active (channel open) A state. The fraction of receptor molecules spontaneously existing in the active state is described by $L = [B]/[A]$. Furthermore, regulation of channel

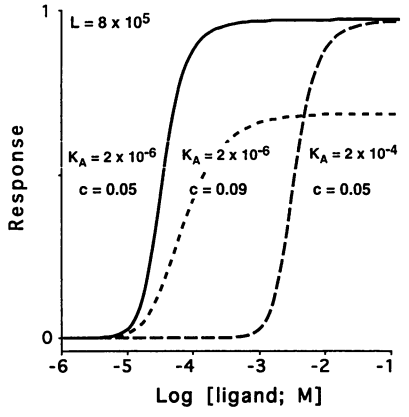

FIG. 2. The *K* phenotype. Theoretical agonist dose–response curves are generated for a two-state B (inactive) $\rightleftharpoons$ A (active) model with equation $\bar{A} = [(1+\alpha)^n]/[(1+\alpha)^n + {}^{BA}L(1+{}^{BA}c\alpha)^n]$, where *n* is the number of sites; α is the concentration of ligand $[X]$ normalized to its affinity for the A state: $\alpha = [X]/K_A$; ${}^{BA}c$ is the ratio of dissociation constants for the B and A states; ${}^{BA}c = K_A/K_B$; and ${}^{BA}L$ is the equilibrium constant between the B and A states in the absence of added ligand: ${}^{BA}L = [B]/[A]$. Values of the parameters *L*, K_A (M) and ${}^{BA}c$ are given. The number of sites is taken to be 5. Equivalent affinity changes for both B and A conformations (modified K_A value, *c* unchanged), result in parallel agonist dose–response curves with no changes in cooperativity or response amplitude. Affinity changes affecting only one conformational state (increased *c* value, *K* unchanged) would alter cooperativity and response amplitude.

opening by an agonist depends on its affinity for the active state, as compared to its affinity for the inactive state ($c = K_A/K_B$). Agonists are characterized by a small value of c, partial agonists by a larger c value, and competitive antagonists by an even larger one. For an L phenotype, as L increases, agonists may progressively become partial agonists and competitive antagonists. For decreasing L values, the reciprocal progression occurs, and, in addition, competitive antagonists may become partial agonists (intermediate c values) or remain competitive antagonists (large c values). Also, in equilibrium binding experiments, apparent affinities will be displaced more for ligands with small c values than for ligands with large c values (Fig. 3). Furthermore, the model predicts that for very small values of L, (*i*) spontaneous stabilization in the active state may occur, yielding constitutively active mutants (spontaneous channel opening), and (*ii*) positive allosteric effectors of the WT, which behave as very weak agonists, may become partial agonists of the mutant. Finally, changes in the L value will generally be accompanied by changes in cooperativity and maximal response amplitude.

Conductance or γ Phenotype. The γ phenotype is assumed to result from changes of the state of activity of the ion channel (e.g., nonconducting to conducting) in one (or possibly more) conformation, with no alteration of the intrinsic binding parameters of each state (i.e., its pharmacological specificity) or of the equilibria (and kinetics) of interconversions. Let us consider that one desensitized conformation, which exhibits high affinity for agonists but has a closed channel, becomes conducting after a mutation. In such a *three-state* model (one activatable and two conducting states), the expected changes of the physiological response properties are 4-fold, as compared to WT: (*i*) desensitization of the response to agonists is reduced because isomerization to a desensitized conformation is no longer accompanied by a closing of the ion channel; (*ii*) the apparent affinity for activation is higher for agonists because desensitized conformations exhibit higher affinity for agonists; (*iii*) a new conducting state, in addition to the WT conducting state, is observed and; (*iv*) the pharmacological drug profile of the two conducting states differ (Fig. 4). Agonists cause the opening of one conducting state at low

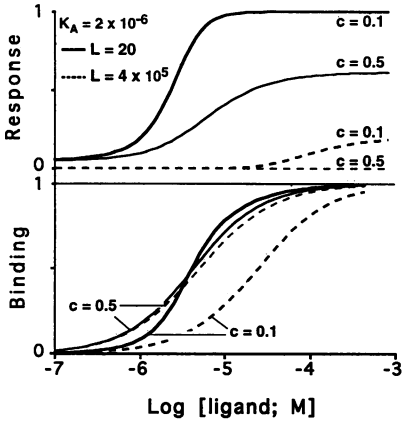

FIG. 3. L phenotype. Theoretical ligand dose–response ($\bar{A}$) and binding-site occupancy ($\bar{Y}$) relations describing the L phenotype. The curves are generated, assuming a two-state B ⇌ A model with five ligand-binding sites, using the equations $\bar{A} = [(1 + \alpha)^n]/[(1 + \alpha)^n + {}^{BA}L(1 + {}^{BA}c\alpha)^n]$ for dose–response curves (*Upper*), and $\bar{Y} = [\alpha (1 + \alpha)^{n-1} + {}^{BA}L\, {}^{BA}c\, \alpha (1 + {}^{BA}c\, \alpha)^{n-1}]/[(1 + \alpha)^n + {}^{BA}L(1 + {}^{BA}c\, \alpha)^n]$ for ligand binding (*Lower*). When the L value decreases from 4×10^5 (broken lines) to 20 (solid lines), (*i*) the agonist ($c = 0.1$) stabilizes the active conformation with increased apparent affinity (lower EC_{50}), efficacy, and cooperativity, as well as with higher apparent binding affinity ($c = 0.1$, *Lower*), whereas (*ii*) the competitive antagonist ($c = 0.5$) becomes a partial agonist (*Upper*) with almost unchanged binding affinity ($c = 0.5$, *Lower*).

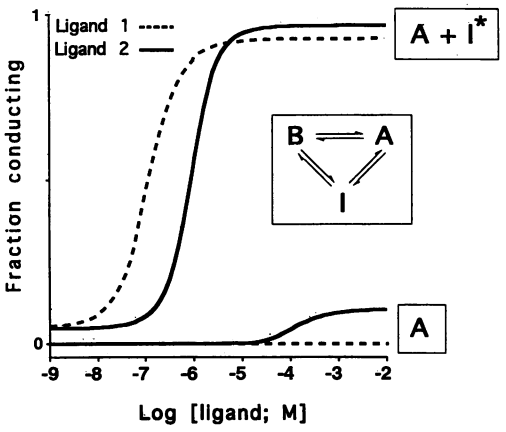

FIG. 4. The γ phenotype. Theoretical dose–response relationships describing the γ phenotype. The curves are generated assuming a three-state model B ⇌ A ⇌ I assuming that either only the A conformation (two-state model) or both the A and I conformations (three-state model) contribute to physiological response. The equation for the three-state model becomes: $\bar{A} + \bar{I} = [(1 + \alpha)^n + {}^{AI}L(1 + {}^{AI}c\,\alpha)^n]/[(1 + \alpha)^n + {}^{AI}L(1 + {}^{AI}c\,\alpha)^n + {}^{AI}L\,{}^{BA}L(1 + {}^{AI}c\,{}^{BA}c\,\alpha)^n]$ with $\alpha = [X]/K_I$. L values for the B ⇌ A transition are ${}^{BA}L = 8 \times 10^5$ and for the A ⇌ I transition ${}^{AI}L = 1.2 \times 10^{-5}$. For ligand 1: $K_A = 2.5 \times 10^{-6}$ M, and ${}^{BA}c = 0.1$, $K_I = 10^{-6}$ M, and ${}^{AI}c = 0.4$. For ligand 2: $K_A = 3.5 \times 10^{-6}$ M and ${}^{BA}c = 0.5$, $K_I = 3 \times 10^{-7}$ M and ${}^{AI}c = 0.0857$. Intrinsic affinities increase from state B to A to I for both ligands. Ligand 1 is a competitive antagonist when the I state corresponds to a closed-channel state and becomes an agonist when the I state has an open channel. Ligand 2, which is an agonist in both cases, stabilizes one or two conducting states depending on the biological activity of the I conformation.

concentration (the high affinity desensitized but conducting state) and of two conducting states at high concentration, whereas competitive antagonists, if stabilizing the desensitized conformation, will activate only the new conducting state at any concentration used.

Complex "Network" Phenotypes. Complex phenotypes will be observed when a large number of conformational states contribute to the physiological response and when mutations affect several conformations simultaneously. Specific predictions of the allosteric model will depend, for each specific receptor, on the number of conformations (and on their intrinsic properties) as well as on their equilibrium constants. Multiple K, L, and/or γ phenotypes may be anticipated. For instance, a network phenotype may be associated with *multiple conducting states* and with mutations changing the number and relative frequencies of opening of several open-channel states.

Experimental Interpretations

Interpretations of ligand-gated ion channel phenotypes rely on a few measurable functional and structural parameters. First, functional parameters generally comprise equilibrium-ligand binding (yielding apparent binding affinities expressed as K_{app} or K_I values with their corresponding Hill coefficients), agonist and competitive antagonist dose–response curves (EC_{50} values, Hill coefficients, response amplitude), and single-channel recordings (single-channel conductance, frequency of channel opening, and mean closed channel time mainly determined over a narrow agonist-concentration range). Yet, little is known to date in mutant receptors about the time course of actual ligand binding and about kinetics of interconversion between conformations. Second, structural parameters obtained by chemical approaches lead to reasonable distinctions among amino acids that compose the ligand-binding area, the ion-channel domain (3, 11), or the lipid–protein boundary (33) and to the estimation of the relative distances of these sites (32, 34). These structural parameters also permit changes in ter-

tiary and quaternary structure to be followed upon stabilization of receptor molecules in different conformations (35–38). However, such data are presently available, almost exclusively from *Torpedo* nicotinic receptor.

Despite the limited information available on these mutants, we may tentatively suggest the following interpretation of their phenotypes in terms of the proposed model.

Nicotinic Receptors Mutated in Their Cholinergic Ligand-Binding Area. The amino acids Tyr-93, Trp-148, Tyr-190, and Tyr-198 were identified by affinity and photoaffinity labeling of the acetylcholine-binding site from the electric organ nicotinic receptor (references in refs. 2, 39). Substitution of their homologs to phenylalanine on chicken neuronal $\alpha 7$ (residues Tyr-92, Trp-148, and Tyr-187; ref. 28) or on mouse muscle $\alpha 1$ subunits (29, 31) yields functional receptors with reduced sensitivity to acetylcholine but unchanged Hill coefficients and maximal current amplitudes. These alterations may be interpreted in terms of a K phenotype, with the intrinsic affinity of the activatable and active conformations being affected to the same extent. As shown in Fig. 5*A*, simulation of $\alpha 7$ nicotinic receptor dose–response curves with changes in solely the K values for Y92F, W148F, and Y187F mutant receptors fits the experimental data points reported in the literature (28) and yield EC_{50} values and Hill coefficients consistent with the experimentally determined values.

Mutations in other parts of the extracellular domain of ligand-gated ion channels alter the pharmacological specificity in a different way. Mutation of Asp-200 in muscle $\alpha 1$ (30) or Gln-198 in neuronal nicotinic $\alpha 3$ (ref. 41, as well as Ile-111 and Ala-212 in $\alpha 1$ glycine receptor subunits; ref. 22), affects the relative affinity and efficacy of distinct agonists. Mutation Asp-200 → Asn, in particular, converts the partial agonists tetramethylammonium and phenyltrimethylammonium into competitive antagonists (30), as expected for changes of intrinsic binding properties of only certain states within the network—i.e., altered c values in a K phenotype. Yet, uncertainties persist about this interpretation because the properties of these mutants may also be accounted for by an L phenotype. Additional experimental data are required to reach a definitive interpretation.

Nicotinic Receptors Mutated in Their Channel Domain. Chemical labeling of *Torpedo* nicotinic receptor with noncompetitive blockers has led to the identification of amino acid rings from the M2 segment of all five subunits that contribute to the channel domain and are conserved in the family of nicotinic receptors (2, 3). In the case of the $\alpha 7$ nicotinic

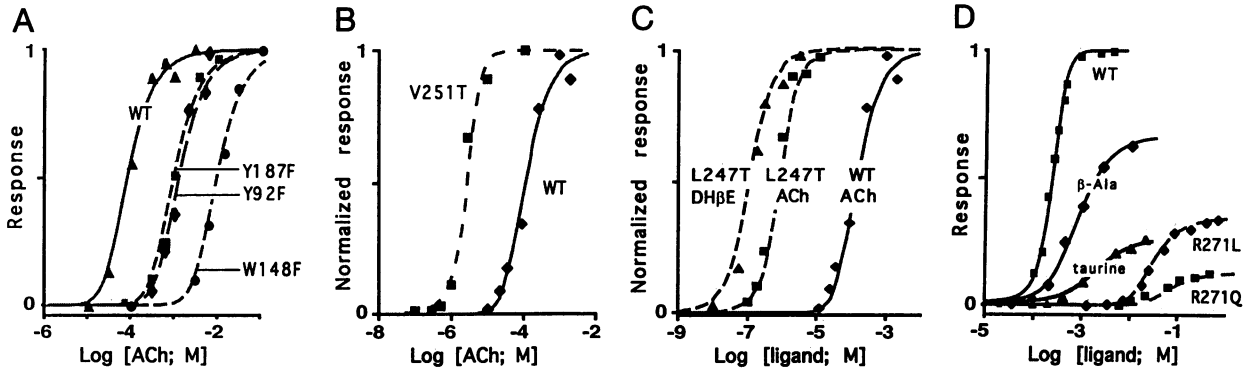

FIG. 5. Experimental interpretations. (*A*) Nicotinic $\alpha 7$ receptor WT and Y92F, W148F, and Y187F mutants as plausible K phenotypes. Values are as follows: $n = 5$, $L = 8 \times 10^5$, and $c = 0.1$. Acetylcholine (ACh) dissociation constants for the active state (K_A, M) are as follows: WT, 2.5×10^{-6}; Y187F, 3×10^{-5}; Y92F, 4×10^{-5}; Y148F, 3×10^{-4}. EC_{50} values are determined as ACh_{50}. Binding cooperativity, expressed as Hill coefficients, is given by $n_H = d \log[\bar{A}_{norm}/(1 - \bar{A}_{norm})]/d \log(\alpha)$, with $\bar{A}_{norm} = [\bar{A} - \bar{A}_{min}]/[\bar{A}_{max} - \bar{A}_{min}]$ and where $\bar{A}_{min} = 1/(1 + {}^{BA}L)$ and $\bar{A}_{max} = 1/(1 + {}^{BA}L\ {}^{BA}c^n)$. Predicted EC_{50} and Hill coefficient values (compared to experimental values from ref. 28 given in parentheses) are as follows: WT, 117 μM and 1.3 (115 μM and 1.7); Y92F, 1.4 mM and 1.3 (1.4 mM and 1.7); W148F, 10.0 mM and 1.3 (10.5 mM and 1.6); Y187F, 1.0 mM and 1.3 (1.2 mM and 1.6). (*B*) The nicotinic receptor $\alpha 7$ V251T mutant as a plausible illustration of the L phenotype. L values for WT and V251T mutant are 8×10^5 and 20, respectively. K_A (2.5×10^{-6} M) and c (0.1) values for acetylcholine, and K_A (3.5×10^{-6} M) and c (0.5) values for DHβE are identical for WT and mutant. Hill coefficients are determined as indicated in *A*. Predicted EC_{50} and Hill coefficient values (compared to experimental values from refs. 14 and 40 given in parentheses) are for acetylcholine on WT: 117 μM and 1.3 (115 μM and 1.4); on V251T, 2.6 μM and 2.1 (2.0 μM and 2.0). Values for DHβE on WT, competitive antagonist; on V251T, partial agonist (I_{max}, 0.6 relative to acetylcholine) $EC_{50} = 9.5$ μM, $n_H = 1.2$ (9.27 μM and 1.4). For correspondence to published data (14, 40) dose–response curves are normalized. However, this simulation accounts for a 10-fold higher maximal acetylcholine response amplitude on V251T than on WT (40). Similar data are obtained for T244Q mutant dose–response curves simulation. (*C*) The $\alpha 7$ nicotinic receptor L247T mutant as a plausible illustration of the γ phenotype. All parameters are identical for WT and mutant. L values are for the B ⇌ A transition ${}^{BA}L = 8 \times 10^5$, and for the A ⇌ I transition ${}^{AI}L = 1.2 \times 10^{-5}$. For acetylcholine, $K_A = 2.5 \times 10^{-6}$ M, ${}^{BA}c = 0.1$, $K_I = 10^{-6}$ M, ${}^{AI}c = 0.4$. For DHβE, $K_A = 3.5 \times 10^{-6}$ M, ${}^{BA}c = 0.5$, $K_I = 3 \times 10^{-7}$ M, ${}^{AI}c = 0.0857$. Hill coefficients for the three-state model are given by $n_H = d \log[\bar{A} + \bar{I}_{norm}/(1 - (\bar{A} + \bar{I})_{norm})]/d \log(\alpha)$, with $\bar{A} + \bar{I}_{norm} = [(\bar{A} + \bar{I}) - (\bar{A} + \bar{I})_{min}]/[(\bar{A} + \bar{I})_{max} - (\bar{A} + \bar{I})_{min}]$ and where $\bar{A} + \bar{I}_{min} = 1/(1 + {}^{BA}L^{AI}L)$ and $\bar{A} + \bar{I}_{max} = 1/(1 + {}^{BA}L\ {}^{BA}c^n\ {}^{AI}L\ {}^{AI}c^n)$. Normalized dose–response curves for acetylcholine and DHβE are fit to experimental data points. Predicted EC_{50} and Hill coefficient values (compared to experimental values from refs. 12–14 given in parentheses) are for acetylcholine on WT:117 μM and 1.3 (115 μM and 1.4); on L247T, 0.6 μM and 2 (0.65 μM and 1.4), and for DHβE on WT, competitive antagonist; on L247T, 0.19 μM and 2.1 (0.18 μM and 1.6). Nonnormalized dose–response curves are similar to those shown in Fig. 4. (*D*) Agonist dose–response relationships for glycine, β-alanine, and taurine (solid lines) on wild-type glycine receptor $\alpha 1$ homooligomers, and for glycine (dashed lines) on R271L and R271Q mutants. Superimposed to experimental data points from ref. 22 are shown the theoretical curves for WT generated by using a two-state B ⇌ A model with $n = 5$. Parameters K_A and c reflecting the intrinsic binding constants for each agonist are adjusted to fit data points, with $L = 100$. For glycine, $K_A = 1.5 \times 10^{-4}$ M and $c = 0.013$; for β-alanine, $K_A = 1.6 \times 10^{-4}$ M and $c = 0.34$; and for taurine, $K_A = 4 \times 10^{-4}$ M and $c = 0.48$. Predicted EC_{50} and n_H values (compared to experimental values from ref. 22 given in parentheses) are for glycine, 0.23 mM and 3 (0.24 mM and 2.9); for β-alanine, 0.79 mM and 1.4 (0.73 mM and 1.6); and for taurine, 2 mM and 1.2 (2.2 mM and 1.3). Glycine dose–response curves on R271L and R271Q mutant receptors are generated by solely changing the allosteric constant L ($L = 1.2 \times 10^9$ for R271L and $L = 2.5 \times 10^9$ for R271Q mutant). To obtain dose–response curves, channel conductances are weighted (conductance × frequency) and normalized to WT "global" channel conductance. The correction factors (1 for WT, 0.5 for R271L mutant, and 0.24 for R271Q mutant) then multiply the $\bar{A}$ state function to yield ionic responses. Predicted EC_{50} and n_H values for glycine (compared to experimental values from ref. 16 given in parentheses) are on R271L, 32 mM and 1.6 (35 mM and 1.7) and on R271Q, 42 mM and 1.5 (44 mM and 1.4). Using the K_A and c values determined for β-alanine and taurine on WT receptor, with the L values determined for the mutants, predicts that these partial agonists no longer elicit ionic responses on mutated receptors but fully occupy ligand-binding sites, as observed for these ligands that are competitive antagonists on mutant receptors (18).

receptor, the available data on the alterations of receptor properties that occur upon substitution of the ring of Val-251 → Thr or of Thr-244 → Gln can be interpreted in terms of L phenotypes. Indeed, acetylcholine dose–response curves can be simulated for WT and mutant receptors with the single assumption that L values are high for the WT ($L = 8 \times 10^5$) and low for the mutants ($L = 20$; see Fig. 5*B*). Such simulation also accounts for the higher maximal amplitudes of ionic response observed for these mutants (14, 40). Furthermore, the competitive antagonist of the WT receptor, DHβE, with its specific binding K and c values (see details in legend to Fig. 5*b*), behaves as a competitive antagonist when the L value corresponds to the WT receptor and as a partial agonist when the L value corresponds to the V251T or T244Q mutant receptor.

Analogies exist between the phenotypes of the M2 mutants L247T and T244Q or V251T. Yet, if the L247T mutant receptor were to correspond to an L phenotype, a single change in L value would *not* fully account for the experimentally determined acetylcholine and DHβE dose–response curves (13, 14). Indeed, with the L value yielding an appropriate EC_{50} for acetylcholine, DHβE will not behave as a full agonist but rather as a partial agonist, as on the T244Q or V251T mutants; moreover, under no circumstances will the apparent affinity for DHβE be, as observed, higher than for acetylcholine. Rather, the occurrence, in addition, in L247T of two conducting states with distinct pharmacological profiles (12–14) favors an interpretation in terms of the γ phenotype scheme. In such a case, simulated acetylcholine and DHβE dose–response curves satisfactorily fit the experimental data (Fig. 5*C*), assuming that one of the conducting states is identical to the WT conducting states (not stabilized by DHβE), whereas the other (assumed to correspond to a desensitized conformation of the WT) binds DHβE with affinity higher than for acetylcholine.

Glycine Receptors Mutated in the Channel Domain. Two mutations identified in M2 from glycine receptor at position R271 (mutations R271L and R271Q) cause the neurological disorder hyperekplexia (42) by drastically reducing the apparent affinity of the receptor for the agonist glycine (16–18). These mutations, in addition, decrease the maximal amplitude of agonist-evoked currents, reduce the number of conducting states when present in the homooligomeric α1 receptors from five (WT) to three (R271L) or one (R271Q), and convert the partial agonists β-alanine and taurine into competitive antagonists. Accordingly, their phenotype appears as a "mirror image" of the phenotypic changes observed in the nicotinic α7 receptor L247T or V251T. The glycine receptor mutants would then resemble wild-type nicotinic acetylcholine receptor. Glycine, β-alanine, and taurine dose–response curves can be simulated for WT homooligomeric α1 glycine receptor, as well as the R271L and R271Q mutants, using, for each ligand, identical binding parameters for WT and mutant receptors and making the minimal assumption that mutations increase L values with the sequence $L_{WT} < L_{R271L} < L_{R271Q}$ (Fig. 5*D*).

To take into account the existence of multiple conducting states (16, 18), glycine dose–response curves were also simulated using an extended "complex network phenotype" scheme comprising several open-channel conformations ^{I}A, ^{II}A, ^{III}A . . ., all in equilibrium with one activatable state. In this scheme, the open-channel states are assumed to exhibit similar quaternary structures (i.e., similar intrinsic binding constants) but distinct single-channel conductances (the state function of each open channel conformation being corrected for conductance differences) and opening frequencies (L values reflecting the relative opening frequencies). The generated curves (data not shown) superimpose with those obtained using the simple two-state model, and changing the binding constants to those of β-alanine or taurine fit their respective reported dose–response relationships.

The experimental data available thus far for the WT and mutant glycine receptor α1 homooligomeric receptors are consistent with the notion that the mutations R271L and R271Q displace the equilibrium between one activatable and one or several active conformations in favor of the activatable state—L value(s) increase(s)—without affecting the intrinsic binding properties of the distinct quaternary structures corresponding to these states. Such an interpretation, in terms of a "complex L phenotype", also accounts for the reported data, indicating that β-alanine and taurine do not desensitize the mutant receptors (18). Yet, further investigation of the pharmacological properties of each detected conducting state is required to determine whether they possess similar or different quaternary structures and, thus, to definitely reject the alternative possibilities.

DISCUSSION

In the present work, we reconsider previously reported mutations in ligand-gated ion channels to clarify the mechanism by which they alter signal transduction in response to neurotransmitter application. The use of the allosteric model, which combines structural information and functional data, leads to specific predictions for mutation phenotypes with altered intrinsic affinity (K), equilibria between conformations (L), or biological activity (γ) of the receptor and accounts for their complex and pleiotropic characters.

In the field of ligand-gated ion channels, the electrophysiological recordings are, most often, conveniently analyzed in terms of a sequential model for channel activation (16, 29, 31). It thus appears challenging to test to what extent this model fits mutant receptor data. This scheme (20) comprises successively a binding step, described by a binding K parameter, and the interconversion of the receptor–agonist complex to an open-channel conformation, with β and α the rate constants for channel opening and closing, respectively. With this formulation, the binding K parameter is identical to the binding constant for the low-affinity activatable state (K_B) of the allosteric scheme, and the α/β ratio is equal to Lc^n in the allosteric scheme. The major difference between the two models thus results from the distinction, in the allosteric model, of an intrinsic equilibrium (L parameter) between interconvertible states that occurs in the absence of ligand and is displaced by the bound ligand as a function of its affinity for one conformation relative to the other (c parameter). The allosteric (but not the sequential) model thus allows the distinction among K phenotypes with altered c values and L phenotypes. The sequential model neither predicts spontaneous channel openings in the absence of ligand (43, 44) nor changes in pharmacological drug profiles, such as those observed in the nicotinic and glycine receptor mutants discussed above. Finally, specific prediction (for patch-clamp recordings) of the allosteric model is that, for K phenotypes, spontaneous channel openings will remain unchanged, but for the L phenotypes, they will be modified.

Specific structural assumptions of the Monod–Wyman–Changeux model have been validated in the case of soluble allosteric enzymes with known three-dimensional structure. Moreover, phenotypes analogous to the K (45), where K refers to allosteric effector affinity, L (9) and γ (46) where γ refers to the catalytic activity, as well as mixed K and L (47) phenotypes, have been described for aspartate transcarbamoylase (K and γ phenotypes), hemoglobin (L phenotype), and phosphofructokinase (mixed K and L phenotypes), among others (for reviews, see refs. 9, 10, 45, 46).

Other neurotransmitter receptors, such as the functionally related glutamate receptors or the structurally unrelated G protein-coupled receptors, exhibit complex functional properties and pleiotropic phenotypes upon mutation. In the case of G protein-coupled receptors, several mutations lead to con-

stitutive activity of the receptor (48), which may result, as discussed here, from (*i*) alteration of the isomerization constant between activatable and active conformations, (*ii*) stabilization of a new conformational state (absent in the WT) with spontaneous biological activity but resistance to desensitization mechanisms, or (*iii*) alteration of the isomerization toward a desensitized conformation. The distinct specific predictions for each possibility would help in designing experiments to further characterize the functional architecture of these receptors. The present speculations may thus be fruitfully extended beyond the ligand-gated ion channels to a wide variety of pharmacological receptors.

We thank P. Ascher, R. Miles, P. Legendre, and M. Kerzberg for critical reading of the manuscript. This work was supported by grants from the Association Française contre les Myopathies, the Collège de France, the Centre National de la Recherche Scientifique, the Institut National de la Santé et de la Recherche Médicale, the Direction de la Recherche Etudes et Techniques, the Commission of the European Communities, and the International Human Frontiers Science Program to J.-P.C. and a grant from the Swiss National Science Foundation to S.J.E.

1. Changeux, J.-P., Devillers-Thiéry, A. & Chemouilli, P. (1984) *Science* **225,** 1335–1345.
2. Devillers-Thiéry, A., Galzi, J. L., Changeux, J.-P., Bertrand, S. & Bertrand, D. (1993) *J. Membr. Biol.* **136,** 97–112.
3. Karlin, A. (1993) *Curr. Opin. Neurobiol.* **3,** 299–309.
4. Kuhse, J., Betz, H. & Kirsch, J. (1995) *Curr. Opin. Neurobiol.* **5,** 318–323.
5. Katz, B. & Thesleff, S. (1957) *J. Physiol. (London)* **138,** 63–80.
6. Heidmann, T. & Changeux, J.-P. (1980) *Biochem. Biophys. Res. Commun.* **97,** 889–896.
7. Neubig, R. R. & Cohen, J. B. (1980) *Biochemistry* **19,** 2770–2779.
8. Monod, J., Wyman, J. & Changeux, J.-P. (1965) *J. Mol. Biol.* **12,** 88–118.
9. Edelstein, S. J. (1975) *Annu. Rev. Biochem.* **44,** 209–232.
10. Perutz, M. F. (1989) *Q. Rev. Biophys.* **22,** 139–236.
11. Galzi, J. L. & Changeux, J.-P. (1994) *Curr. Opin. Struct. Biol.* **4,** 554–565.
12. Revah, F., Bertrand, D., Galzi, J. L., Devillers-Thiéry, A., Mulle, C., Hussy, N., Bertrand, S., Ballivet, M. & Changeux, J.-P. (1991) *Nature (London)* **353,** 846–849.
13. Bertrand, D., Devillers-Thiéry, A., Revah, F., Galzi, J. L., Hussy, N., Mulle, C., Bertrand, S., Ballivet, M. & Changeux, J.-P. (1992) *Proc. Natl. Acad. Sci. USA* **89,** 1261–1265.
14. Devillers-Thiéry, A., Galzi, J. L., Bertrand, S., Changeux, J.-P. & Bertrand, D. (1992) *NeuroReport* **3,** 1001–1004.
15. Yakel, J. L., Lagrutta, A., Adelaman, J. P. & North, R. A. (1993) *Proc. Natl. Acad. Sci. USA* **90,** 5030–5033.
16. Langosh, D., Laube, B., Rundström, N., Schmieden, V., Bormann, J. & Betz, H. (1994) *EMBO J.* **13,** 4223–4228.
17. Rajendra, S., Lynch, J., Pierce, K. D., French, C. R., Barry, P. H. & Schofield, P. R. (1994) *J. Biol. Chem.* **269,** 18739–18742.
18. Rajendra, S., Lynch, J., Pierce, K. D., French, C. R., Barry, P. H. & Schofield, P. R. (1995) *Neuron* **14,** 169–175.
19. Labarca, C., Nowak, M. W., Zhang, H., Tang, L., Desphande, P. & Lester, H. A. (1995) *Nature (London)* **376,** 514–516.
20. Del Castillo, J. & Katz, B. (1957) *Proc. R. Soc. London Ser. B* **146,** 369–381.
21. Luetje, C. W. & Patrick, J. (1991) *J. Neurosci.* **11,** 837–845.
22. Schmieden, V., Kuhse, J. & Betz, H. (1992) *EMBO J.* **11,** 2025–2032.
23. Role, L. W. (1992) *Curr. Opin. Neurobiol.* **2,** 254–262.
24. Bertrand, D., Galzi, J. L., Devillers-Thiéry, A., Bertrand, S. & Changeux, J.-P. (1993) *Proc. Natl. Acad. Sci. USA* **90,** 6971–6975.
25. Cachelin, A. B. & Jaggi, R. (1991) *Pfluegers Arch.* **419,** 579–582.
26. Bormann, J., Rundström, N., Betz, H. & Langosh, D. (1993) *EMBO J.* **12,** 3729–3737.
27. Sakmann, B., Patlak, J. & Neher, E. (1980) *Nature (London)* **286,** 71–73.
28. Galzi, J. L., Bertrand, D., Devillers-Thiéry, A., Revah, F., Bertrand, S. & Changeux, J.-P. (1991) *FEBS Lett.* **294,** 198–202.
29. Tomaselli, G. F., McLaughlin, J. T., Jurman, M., Hawrot, E. & Yellen, G. (1991) *Biophys. J.* **60,** 721–727.
30. O'Leary, M. E. & White, M. M. (1992) *J. Biol. Chem.* **267,** 8360–8365.
31. Aylwin, M. L. & White, M. M. (1994) *Mol. Pharmacol.* **46,** 1149–1155.
32. Herz, J. M., Johnson, D. A. & Taylor, P. (1989) *J. Biol. Chem.* **264,** 12439–124448.
33. Blanton, M. P. & Cohen, J. B. (1994) *Biochemistry* **33,** 2859–2872.
34. Valenzuela, C. F., Weign, P., Yguerabide, J. & Johnson, D. A. (1994) *Biophys. J.* **66,** 674–682.
35. Galzi, J. L., Revah, F., Bouet, F., Ménez, A., Goeldner, M., Hirth, C. & Changeux, J.-P. (1991) *Proc. Natl. Acad. Sci. USA* **88,** 5051–5055.
36. White, B. J. & Cohen, J. B. (1992) *J. Biol. Chem.* **267,** 15770–15783.
37. Unwin, N. (1995) *Nature (London)* **373,** 37–43.
38. Unwin, N., Toyoshima, C. & Kubalek, E. (1988) *J. Cell Biol.* **107,** 1123–1138.
39. Corringer, P. J., Galzi, J. L., Eiselé, J. L., Bertrand, S., Changeux, J.-P. & Bertrand, D. (1995) *J. Biol. Chem.* **270,** 11749–11752.
40. Galzi, J. L., Devillers-Thiery, A., Hussy, N., Bertrand, S., Changeux, J.-P. & Bertrand, D. (1992) *Nature (London)* **359,** 500–505.
41. Luetje, C. W., Piattoni, M. & Patrick, J. (1993) *Mol. Pharmacol.* **44,** 657–666.
42. Shiang, R., Ryan, S. G., Zhu, Y. Z., Hahn, A. F., O'Connell, P. & Wasmuth, J. J. (1993) *Nat. Genet.* **5,** 351–358.
43. Jackson, M. B. (1984) *Proc. Nat. Acad. Sci. USA* **81,** 3901–3904.
44. Ohno, K., Hutchison, D. O., Milone, M., Brengham, J. M., Bouzat, C., Sine, S. M. & Engel, A. G. (1995) *Proc. Natl. Acad. Sci. USA* **92,** 758–762.
45. Kantrowitz, E. R. & Lipscomb, W. N. (1988) *Science* **241,** 669–674.
46. Schachman, H. K. (1988) *J. Biol. Chem.* **263,** 18583–18586.
47. Berger, S. A. & Evans, P. R. (1990) *Nature (London)* **343,** 575–576.
48. Lefkowitz, R., Cotecchia, S., Samama, P. & Costa, T. (1993) *Trends Pharmacol. Sci.* **14,** 303–307.